

Control of axon–axon attraction by Semaphorin reverse signaling

Hsiao-Han Hsieh^{a,b}, Wen-Tzu Chang^a, Li Yu^a, and Yong Rao^{a,c,1}

^aMcGill Centre for Research in Neuroscience, Department of Neurology and Neurosurgery, ^cDepartment of Medicine, and ^bDepartment of Biology, McGill University Health Centre, Montreal, QC, Canada H3G 1A4

Edited by Alex L. Kolodkin, The Johns Hopkins University School of Medicine, Baltimore, MD, and accepted by the Editorial Board June 27, 2014 (received for review November 18, 2013)

Semaphorin family proteins are well-known axon guidance ligands. Recent studies indicate that certain transmembrane Semaphorins can also function as guidance receptors to mediate axon–axon attraction or repulsion. The mechanisms by which Semaphorin reverse signaling modulates axon-surface affinity, however, remain unknown. In this study, we reveal a novel mechanism underlying upregulation of axon–axon attraction by Semaphorin-1a (Sema1a) reverse signaling in the developing *Drosophila* visual system. Sema1a promotes the phosphorylation and activation of Moesin (Moe), a member of the ezrin/radixin/moesin family of proteins, and downregulates the level of active Rho1 in photoreceptor axons. We propose that Sema1a reverse signaling activates Moe, which in turn upregulates Fas2-mediated axon–axon attraction by inhibiting Rho1.

The Semaphorin family of proteins are well-known axon guidance cues or ligands, which activate their receptors on a variety of axons to control axonal pathfinding, fasciculation, branching, and target selection in vertebrates and invertebrates (1, 2). Recent studies demonstrate that certain transmembrane Semaphorins can also function as a receptor to mediate downstream signaling events in both vertebrates and invertebrates (3–7). For example, we show that the transmembrane Semaphorin-1a (Sema1a) functions as an axon guidance receptor for PlexinA (PlexA) in mediating reverse signaling in the developing *Drosophila* visual system (3, 8). Sema1a reverse signaling promotes photoreceptor (R cell) axon–axon attractions during the establishment of R-cell-to-optic-lobe connections (8). A recent study by Kolodkin and colleagues also demonstrates that Sema1a reverse signaling mediates axon–axon repulsion in *Drosophila* motor axon guidance (6).

To understand the mechanisms underlying upregulation of axon–axon attractions by Sema1a reverse signaling, we set out to examine potential genetic interactions between Sema1a and other genes in R-cell axon guidance. The establishment of R-cell-to-optic-lobe connections in the *Drosophila* adult visual system begins at the third-instar larval stage (9). At the third-instar larval stage, differentiating R cells in the eye-imaginal disk extend axons through the optic stalk into the developing optic lobe. R1–R6 axons terminate at the superficial lamina layer, where their growth cones closely associate with each other at the lamina termination site. R7 and R8 axons bypass the lamina and terminate in the deeper medulla layer.

In this study, we present evidence that Sema1a reverse signaling promotes R-cell axon–axon attraction by upregulating the adhesive function of Fasciclin 2 (Fas2). Sema1a interacts genetically and physically with Moesin (Moe), a member of the ezrin/radixin/moesin (ERM) family proteins, and downregulates the level of active Rho1. Our results support that Sema1a-induced reduction in the level of active Rho1 in R-cell axons contributes to an increase in Fas2-mediated R-cell axon–axon attraction.

Results

Sema1a Interacts with Fas2 in Regulating R-Cell Axonal Projections.

In our previous study (3), we showed that hyper-activation of Sema1a reverse signaling by Sema1a overexpression induces

hyper-fasciculation of R-cell axons (Fig. 1*B*). To identify other components of the Sema1a reverse-signaling pathway, we tested if reducing the level of other genes (i.e., candidate genes encoding cell-surface receptors and intracellular signaling proteins) modifies the Sema1a hyper-activation phenotype. Interestingly, we found that eye-specific knockdown of *Fas2* significantly suppressed the hyper-fasciculation phenotype induced by *sema1a* overexpression (Fig. 1*C* and *D* and *SI Appendix*, Fig. *S1*), suggesting that *Fas2* is a downstream target of Sema1a reverse signaling. Consistently, we found that *Fas2*, like Sema1a (3), is present in R-cell axons (*SI Appendix*, Fig. *S2*).

Sema1a Promotes Fas2-Mediated Cell–Cell Adhesion. To determine the mechanisms underlying the observed genetic interaction between *Fas2* and Sema1a, we performed cell culture study. Expression of *Fas2*-YFP in the *Drosophila* Schneider-2 cells (S2 cells) induced the formation of large homotypic cell aggregates (>20 cells) (Fig. 2*B* and *E*), whereas cells transfected with YFP expression construct did not form large cell aggregates (Fig. 2*A* and *E*). We found that expression of Sema1a greatly enhanced *Fas2*-mediated cell–cell adhesion (Fig. 2*C* and *E*). To determine domain requirements, we tested a truncated Sema1a mutant (i.e., Sema1a^{ΔCyt0}) in which a large portion of the cytoplasmic domain was deleted. Although Sema1a^{ΔCyt0} was still capable of binding to PlexA (*SI Appendix*, Fig. *S3*), it did not enhance *Fas2*-mediated cell–cell aggregation (Fig. 2*D* and *E*). This result indicates that Sema1a uses its cytoplasmic domain to activate downstream signaling events, which then upregulate the adhesive function of *Fas2*.

Loss of *Fas2* Causes a *sema1a*-Like Phenotype. To examine if *Fas2*, like Sema1a, is required for R-cell axon–axon association in the developing optic lobe, we performed loss-of-function analysis. In wild type (Fig. 3*A* and *SI Appendix*, Fig. *S4A*), differentiating R cells project axons through the optic stalk into the optic lobe. R1–R6

Significance

Bidirectional signaling between ligand and receptor facilitates cell–cell communication. Recent studies show that members of the well-known Semaphorin family proteins can mediate both forward and reverse signaling in regulating neural network formation. In this study, we identify new components of the Semaphorin reverse signaling pathway and reveal a novel mechanism by which Semaphorin reverse signaling promotes axon–axon attraction in patterning neuronal circuitry during development.

Author contributions: H.-H.H., W.-T.C., L.Y., and Y.R. designed research; H.-H.H., W.-T.C., and L.Y. performed research; H.-H.H., W.-T.C., L.Y., and Y.R. analyzed data; and H.-H.H. and Y.R. wrote the paper.

The authors declare no conflict of interest.

This article is a PNAS Direct Submission. A.L.K. is a guest editor invited by the Editorial Board.

¹To whom correspondence should be addressed. Email: yong.rao@mcgill.ca.

This article contains supporting information online at www.pnas.org/lookup/suppl/doi:10.1073/pnas.1321433111/-DCSupplemental.

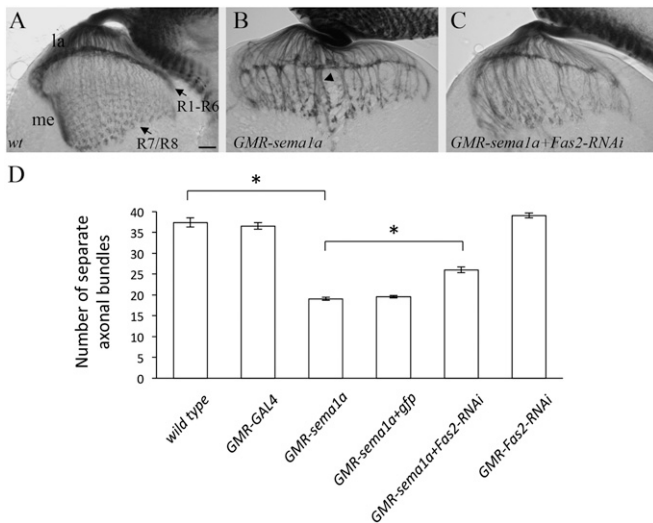


Fig. 1. *sema1a* interacts genetically with *Fas2* in R-cell axonal projections. (A) In wild-type third-instar larvae, R1–R6 growth cones form a smooth layer in the lamina intermediate target region. R7 and R8 axons extend into the medulla. (B) In flies overexpressing *Sema1a* in R-cell axons, R-cell axons formed thicker bundles (arrowhead). (C) Knockdown *Fas2* in flies overexpressing *Sema1a* partially suppressed the hyper-fasciculation phenotype. Note that many individual axons also displayed defects at the R1–R6 terminal layer. (D) The data were quantified by examining R-cell axonal projections in third-instar larvae with comparable eye-disk size (more than 10 rows of differentiating R-cell clusters). The number of separate axonal bundles that were located between lamina and medulla was counted. Overexpression of *Sema1a* induced the formation of thicker bundles and thus decreased the number of separate R-cell axonal bundles. * $P < 0.001$. la, lamina; me, medulla. (Scale bar, 20 μm .) Error bars: SEM.

axons terminate in the superficial lamina layer, where their growth cones associate closely with each other to form a dense and smooth layer at the lamina termination site. R7 and R8 axons extend through the lamina into the deeper medullar layer, where their growth cones expand significantly in size. In our previous studies (3), we showed that loss of *Sema1a* reverse signaling disrupts R-cell axon–axon association, leading to the appearance of many gaps at the lamina termination layer and frequently dispersed distribution of R-cell axonal terminals (~72.7%, $n = 11$; Fig. 3B and *SI Appendix*, Fig. S4B and C). We performed eye-specific genetic mosaic analysis to generate large clones of homozygous *Fas2* mutant cells in third-instar eye discs (Fig. 3C). Like *sema1a* mutants (Fig. 3B), *Fas2* eye-specific mosaic animals displayed a discontinuous and loose R-cell lamina termination layer (~70%, $n = 50$; Fig. 3C and *SI Appendix*, Fig. S4D). A similar phenotype was also observed when *Fas2* was knocked down in R-cell axons (~79.3%, $n = 29$; Fig. 3D and *SI Appendix*, Fig. S2C).

To further investigate the functional relationship between *Sema1a* and *Fas2*, we examined if loss of *sema1a* affects the level of *Fas2* in R-cell axons. Compared with that in wild type (*SI Appendix*, Fig. S5)—although there was a decrease in *Fas2* level in R7/R8 terminals in *sema1a* mutants—no such change was observed in R1–R6 terminals in *sema1a* mutants (*SI Appendix*, Fig. S5). Interestingly, although overexpression of *Fas2* in wild type caused a hyper-fasciculation phenotype similar to that of *Sema1a* overexpression, no hyper-fasciculation phenotype was observed when *Fas2* was overexpressed in *sema1a* mutants (*SI Appendix*, Fig. S6). Moreover, many *sema1a* mutants in which *Fas2* was overexpressed still displayed defects similar to those in *sema1a* mutants (~72.2%, $n = 18$). These results, together with the fact that *Sema1a* promotes *Fas2*-mediated cell–cell adhesion in S2 cells (Fig. 2), suggest a role for *Sema1a* in upregulating the adhesive activity and/or stability of *Fas2*.

Sema1a Downregulates the Level of Active Rho1 in R-Cell Axons. To elucidate the signaling events underlying upregulation of *Fas2* by *Sema1a*, we tested candidate intracellular signaling proteins for a potential role in the *Sema1a* reverse-signaling pathway. Among them, Rho1 is a particularly attractive candidate. In our previous study (8), we presented genetic evidence supporting that *Sema1a* reverse signaling negatively regulates Rho1 in controlling R-cell axonal projections. To gain mechanistic insights into negative regulation of Rho1 by *Sema1a* reverse signaling, we examined the effects of manipulating the level of *Sema1a* on the activation of Rho1 in R-cell axons in the developing *Drosophila* visual system.

The distribution of active Rho1 was monitored with the Rho1 sensor PKNG58AeGFP (PKN-GFP). PKN-GFP binds to active Rho1 (i.e., GTP-bound form) and has been used to follow Rho1 activation (10). The relative level of active Rho1 (i.e., axon versus R-cell bodies in the eye disk) was measured. Loss of *sema1a* led to a significant increase in the level of active Rho1 in R-cell axons (Fig. 4B and C). Conversely, overexpression of *Sema1a* decreased the level of active Rho1 in R-cell axons (Fig. 4C). These results indicate that *Sema1a* downregulates the level of active Rho1 in R-cell axons.

Rho1 Inhibits Fas2-Mediated Cell–Cell Adhesion. To test if Rho1 plays a role in regulating the function of *Fas2*, we examined the effects of manipulating the activity of Rho1 on *Fas2*-mediated cell–cell adhesion. The activity of Rho1 in cultured cells was manipulated by expressing constitutively active (i.e., Rho1V14) or dominant-negative (i.e., Rho1N19) forms of Rho1. Although increasing Rho1 activity by expressing the constitutively active Rho1V14 abolished *Fas2*-mediated cell–cell aggregation (Fig. 4D), downregulating Rho1 activity with Rho1N19 significantly enhanced *Fas2*-mediated cell adhesion (Fig. 4D).

Rho1 Activation Decreases the Surface Level of Fas2. To determine the mechanisms by which Rho1 inhibits *Fas2*, we examined the effects of Rho1 on the distribution pattern of *Fas2*. In S2 cells transfected with *Fas2*-YFP alone (Fig. 5A and B), *Fas2* showed continuous cell-surface staining. In S2 cells expressing both *Fas2*-YFP and Rho1V14 (Fig. 5A and B), however, the surface presence of *Fas2* was significantly reduced. Many cells displayed discontinuous surface distribution of *Fas2*, coincident with the appearance of vesicle-like particles within the cytoplasm. We also tested the effects of Rho1 activation on several other cell-surface receptors, but did not observe a similar decrease in their

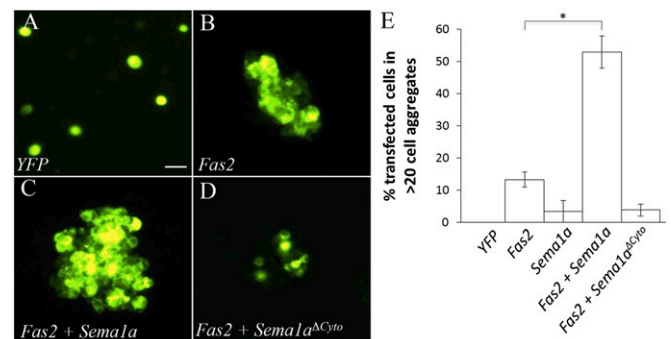


Fig. 2. *Sema1a* enhances *Fas2*-mediated cell–cell adhesion. (A) Cells transfected with YFP expression construct did not form large cell aggregates (i.e., an aggregate with the size of >20 cells). (B) Cells expressing *Fas2*-YFP formed large cell aggregates (>20 cells). (C) Coexpression of *Sema1a* greatly increased the frequency of *Fas2*-induced cell aggregates and the size of aggregates. (D) Coexpression of a *Sema1a* mutant lacking a large portion of the cytoplasmic domain did not enhance *Fas2*-induced cell–cell aggregation. (E) The percentage of *Fas2*-positive cells that formed large cell aggregates (>20 cells) were quantified. The bar for YFP-transfected cells did not show up as no large cell aggregate (>20 cells) was observed. * $P = 0.0019$. (Scale bar, 20 μm .) Error bars: SEM.

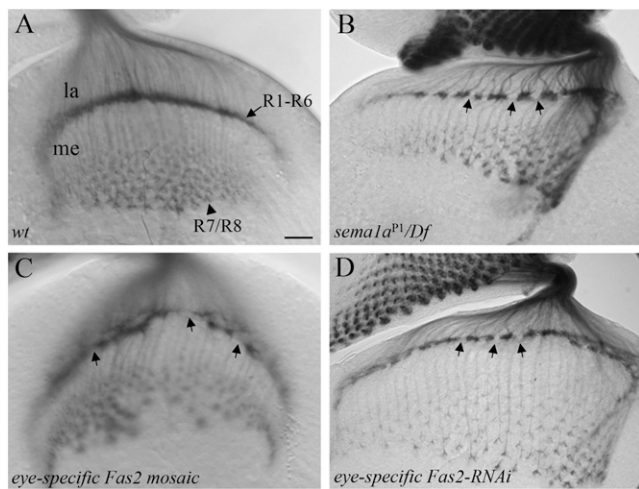


Fig. 3. Loss of *Fas2* disrupts R-cell axon-axon association. (A) Wild type. (B) In mutants defective in *Sema1a* reverse signaling [e.g., *sema1a^{P1}/Df(2L)BSC204*], R-cell axons displayed defects in axon-axon attraction, leading to the appearance of many gaps (more than three; arrows) at the lamina intermediate target region. (C) In *Fas2* null mutant (i.e., *Fas2^{EB112}*) eye-specific mosaic animals, gaps (arrows) at the lamina target region were frequently observed. (D) In *Fas2* eye-specific knockdown animals, similar disruption at the lamina target region was observed. The arrows indicate gaps at the lamina termination layer. la, lamina; me, medulla. (Scale bar, 20 μ m.)

surface levels (SI Appendix, Fig. S7). These results indicate that Rho1 negatively regulates *Fas2*-mediated cell-cell adhesion by decreasing the surface level of *Fas2*.

To determine the mechanisms by which Rho1 activation leads to a decrease in the surface level of *Fas2*, we examined the effects of Rho1 activation on intracellular trafficking of *Fas2*. Expression of Rho1V14 significantly increased the localization of *Fas2* to intracellular vesicles positive for *Drosophila* Dynamin (i.e., Shibire) (Fig. 5 C and D), a key component of the endocytic pathway (11). By contrast, no increase was observed in colocalization of *Fas2* with Rab11 (SI Appendix, Fig. S8), a key player in the recycling endosome pathway (12). Expression of Rho1V14 also significantly increased the colocalization of *Fas2* with vesicles positive for Rab7 (Fig. 5 E and F), which plays an important role in regulating late endosome/lysosome trafficking (12). These results suggest that Rho1 activation decreases the surface level of *Fas2* by promoting intracellular trafficking and degradation of *Fas2*.

Sema1a Interacts Physically and Genetically with Moe. To determine the mechanisms by which *Sema1a* regulates the level of active Rho1, we tested the potential interaction between *Sema1a* and Moe, a member of the ERM family of proteins that was reported to be a negative regulator of Rho1 in *Drosophila* epithelial morphogenesis (13). A Glutathione-S (GST) fusion protein containing the cytoplasmic domain of *Sema1a* (GST-Cyto) was used in GST pull-down experiments. GST-Cyto, but not GST, precipitated Moe from fly lysates (Fig. 6A). This result suggests that *Sema1a* binds to Moe. To further address this, we performed coimmunoprecipitation. We found that *Sema1a*-GFP could coprecipitate with Moe-FLAG in transfected S2 cells (Fig. 6B). Coprecipitation was substantially reduced when a portion of the cytoplasmic domain of *Sema1a* was deleted (Fig. 6B). These results suggest that *Sema1a* associates with Moe to promote axon-axon interactions in the developing *Drosophila* visual system.

To determine the *in vivo* relevance of the association of *Sema1a* with Moe, we examined potential genetic interactions between *Sema1a* and Moe in R-cell axonal projections. We found that the knockdown the level of Moe significantly suppressed the hyper-fasciculation phenotype induced by *Sema1a* overexpression (Fig. 6C and SI Appendix, Fig. S9), whereas overexpression of Moe enhanced the *Sema1a* overexpression

phenotype (Fig. 6C and SI Appendix, Fig. S9). We also found that reducing the level of *Fas2* suppressed the hyper-fasciculation phenotype induced by expressing a constitutively active form of Moe (i.e., Moe^{T559D}) (SI Appendix, Fig. S10) or a dominant-negative form of Rho1 (i.e., Rho1N19) (SI Appendix, Fig. S10).

Sema1a Is Required for the Phosphorylation and Activation of Moe in R-Cell Axons. To further determine the functional relationship between *Sema1a* and Moe, we examined the effects of manipulating the level of *Sema1a* on the level and activation of Moe in R-cell axons in the developing *Drosophila* visual system. Because Moe is expressed in all cell types in the developing visual system, the presence of Moe in individual R-cell bodies and axons could not be unequivocally identified (SI Appendix, Fig. S11C). To circumvent this problem, we performed immunostaining of dissociated R cells from third-instar larval eye discs (SI Appendix, Fig. S11D). The expression level of total Moe was examined with a rabbit anti-Moe antibody (14), whereas the level of active Moe (i.e., pMoe) that is phosphorylated on Thr556 was examined with a rabbit anti-pMoe antibody (15) (SI Appendix, Fig. S12). The relative level of total Moe and pMoe in R-cell bodies and axons was quantified. Loss of *sema1a* did not affect the relative level of total Moe in R-cell bodies and axons (Fig. 7 G, H, and J), indicating that *Sema1a* reverse signaling is not required for transcription or translation of Moe. The relative level of phosphorylated Moe, however, was decreased substantially in the absence of *Sema1a* (Fig. 7 C, D, and J). We also found that Moe is involved in downregulating the level of active Rho1 in dissociated R-cell axonal terminals (SI Appendix, Fig. S13) and in R1-R6 terminals in the developing *Drosophila* visual system (SI Appendix, Fig. S14). These results indicate that *Sema1a* reverse

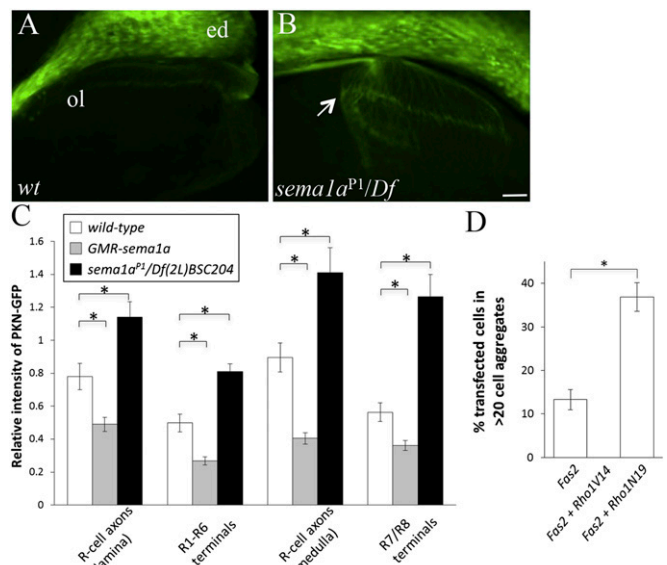


Fig. 4. *Sema1a* downregulates the level of active Rho1 in R-cell axons. (A–C) PKN-GFP was used to visualize and quantify the level of active Rho1 in R cells. (A) The distribution of PKN-GFP in wild-type third-instar eye-brain complexes. (B) In *sema1a^{P1}/Df(2L)BSC204* mutants, the level of PKN-GFP in R-cell axons was increased significantly. Arrow indicates R-cell axons. (C) The relative level of active Rho1 was quantified. The relative intensity of PKN-GFP at different segments of R-cell axons was calculated by measuring the ratio of PKN-GFP intensity in R-cell axonal segments versus that in R-cell bodies in the same eye disk. **P* < 0.01. (D) The effects of manipulating the activity of Rho1 on *Fas2*-induced cell-cell aggregation were examined. The percentage of *Fas2*-positive cells that formed large cell aggregates were quantified. The bar for cells coexpressing *Fas2* and Rho1V14 did not show up as no large cell aggregates (>20 cells) were observed. By contrast, expression of Rho1N19 greatly enhanced *Fas2*-mediated cell aggregation (**P* = 0.0028). ed, eye disk; ol, optic lobe. (Scale bar, 20 μ m.) Error bars: SEM.

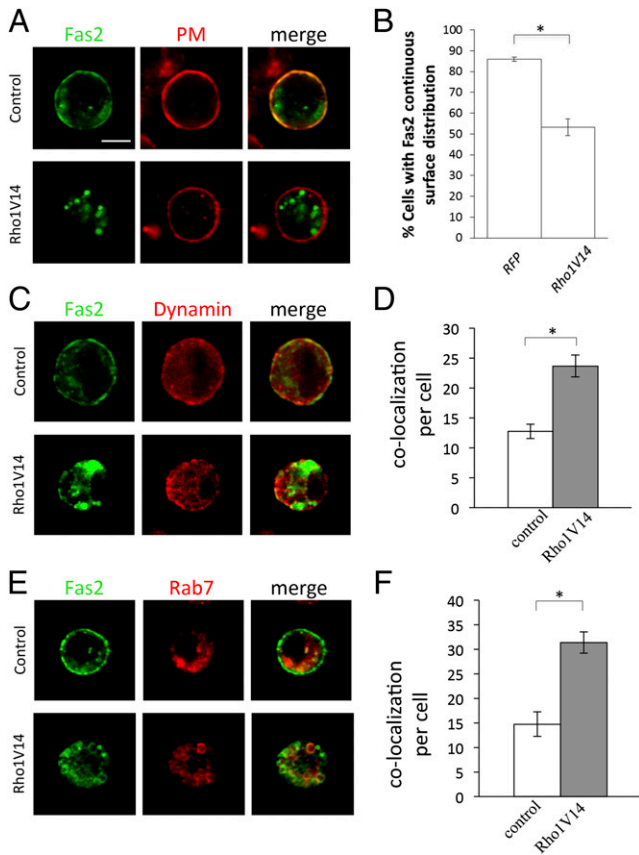


Fig. 5. Rho1 downregulates the surface level of Fas2 in cultured cells. (A) S2 cells expressing Fas2-YFP (Upper) or both Fas2-YFP and Rho1V14 (Lower) were labeled with CellMask Plasma Membrane Stains (Life Technologies) to visualize plasma membrane (PM). Cells expressing Fas2-YFP displayed continuous cell-surface distribution of Fas2. However, many cells coexpressing Fas2-YFP and Rho1V14 showed disruptions in surface distribution of Fas2, which was coincidentally with an increase in the intracellular presence of Fas2. (B) The percentage of cells showing continuous surface distribution of Fas2 was quantified. $*P = 0.0013$. (C) S2 cells expressing Fas2-YFP (Upper) or both Fas2-YFP and Rho1V14 (Lower) were stained with anti-Dynamin antibody (red). Compared with that in control cells (Upper) ($n = 15$), the number of vesicles positive for both Fas2 (green) and Dynamin (red) were significantly increased in Rho1V14-expressing cells ($n = 18$). (D) The number of vesicles that were colabeled by anti-Dynamin and YFP in each cell was quantified. $*P = 3.71E-05$. (E) S2 cells expressing Fas2-YFP and Rab7-HA (Upper) or Fas2-YFP, Rab7-HA, and Rho1V14 (Lower) were colabeled with YFP fluorescence (green) and anti-HA (red). Compared with that in control cells (Upper) ($n = 15$), the number of vesicles positive for both Fas2-YFP and Rab7-HA was significantly increased in Rho1V14-expressing cells ($n = 14$). (F) The number of vesicles that were colabeled by Fas2-YFP and Rab7-HA in each cell was quantified. $*P = 3.02E-05$. (Scale bar, 5 μ m.) Error bars: SEM.

signaling negatively regulates Rho1 by promoting the activation of Moe in R-cell axons.

Loss of *moe* also Disrupts the Association of R-Cell Axons. To determine if Moe is required for R-cell axon-axon association, we performed loss-of-function analysis. The level of both phosphorylated Moe and total Moe protein was significantly reduced in *moe*^{G0323} mutants and *moe* knockdown flies (SI Appendix, Figs. S11 and S12). Similar to that in *sema1a* mutants (Fig. 7L), the close association of R-cell axons at the lamina termination layer was disrupted in *moe*^{G0323} mutants (~66.7%, $n = 21$; Fig. 7M), and larvae in which the level of Moe was knocked down by eye-specific expression of a *UAS-moe-RNAi* transgene (~50%, $n = 22$; Fig. 7N). Together, these results support a role for Moe in

the *Sema1a* reverse-signaling pathway in regulating R-cell axon-axon interactions.

Discussion

Our previous studies establish a key role for *Sema1a* reverse signaling in promoting R-cell axon-axon association at the intermediate target region in the developing visual system (3, 8). In this study, we reveal a novel mechanism underlying modulation of axon-surface affinity by *Sema1a* reverse signaling. Our results implicate the homophilic cell adhesion molecule Fas2 as a downstream target of *Sema1a* reverse signaling. We show that the *Sema1a*-induced axonal hyper-fasciculation phenotype is suppressed by reducing the level of Fas2. Loss of *Fas2* disrupts the association of R-cell axons in the lamina, a phenotype similar to that in *sema1a* mutants. Consistently, we found that expression of *Sema1a*, but not of the *Sema1a* mutant lacking the cytoplasmic domain, enhances Fas2-mediated cell-cell adhesion in vitro. We propose that upregulation of Fas2-mediated axon-axon attraction by *Sema1a* reverse signaling is a key step in organizing R-cell axons at their intermediate target region before establishing synaptic connections with their final target neurons in the optic lobe.

Our results revealing the regulation of Fas2 by *Sema1a* reverse signaling shed new light on the mechanisms controlling axon-axon interactions in circuit development. Fas2 and its mammalian ortholog NCAM have been implicated in a variety of processes in neural development and function, such as axon guidance, synaptic development, and plasticity (16). The function of Fas2/

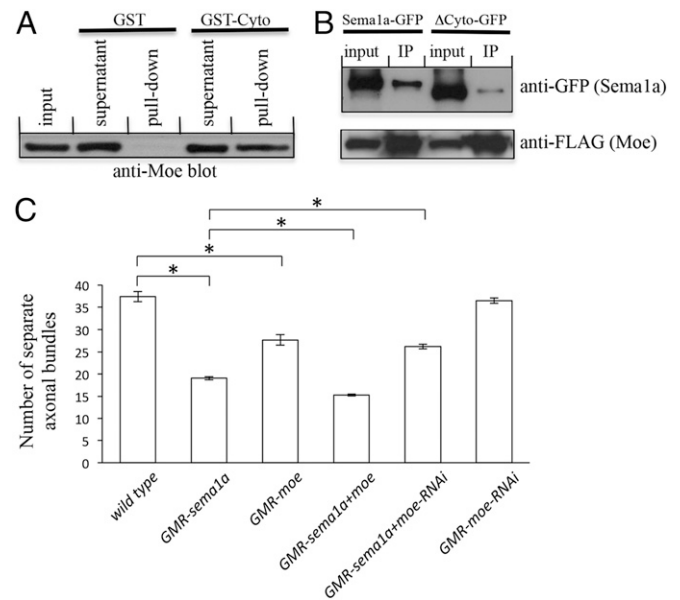


Fig. 6. *Sema1a* interacts physically and genetically with Moe. (A) Western blot analysis of precipitates pulled down from lysates of flies expressing Moe-Myc by GST or GST fusion protein containing the cytoplasmic domain of *Sema1a* (i.e., GST-Cyto). Moe was detected in GST-Cyto precipitates, but not in GST precipitates. (B) Anti-FLAG antibody was used to precipitate Moe-FLAG from S2 cells coexpressing Moe-FLAG and *Sema1a*-GFP or Moe-FLAG and Δ Cyto-GFP (*Sema1a* mutant lacking a portion of the cytoplasmic domain). (Upper) The blot was probed with anti-GFP antibody. (Lower) The same blot was stripped and reprobed with anti-FLAG antibody. (C) The effects of manipulating the level of Moe on the *Sema1a*-overexpression-induced hyper-fasciculation phenotype were quantified. Third-instar larvae with comparable eye-disk size (more than 10 rows of differentiating R-cell clusters) were examined, and the number of separate axonal bundles that are located between lamina and medulla was counted. The *Sema1a*-overexpression-induced hyper-fasciculation phenotype was enhanced by overexpression of Moe and suppressed by knockdown of Moe. $*P < 0.001$. Error bars: SEM.

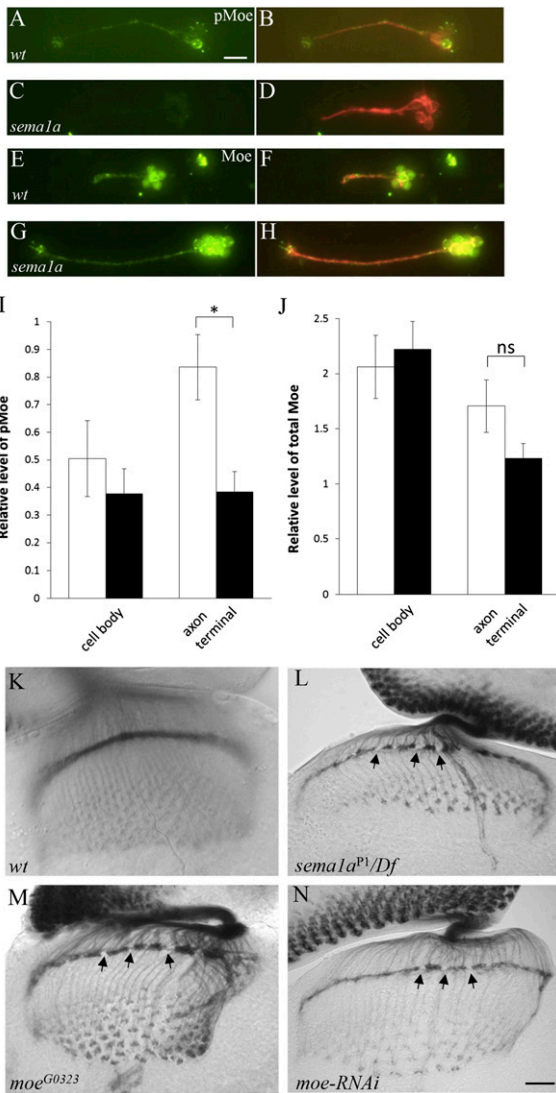


Fig. 7. *Sema1a* is required for the phosphorylation and activation of Moe in R-cell axons. (A–H) Dissociated R cells from third-instar eye discs were cultured. (A–D) The distribution of phosphorylated active Moe (pMoe) was visualized with anti-phosphorylated Moe antibody. (A) Phosphorylated Moe was detected in wild-type R-cell bodies and axons. (B) R cells in A were double-stained with R-cell-specific monoclonal antibody MAb 24B10. (C) In *sema1a^{P1}/Df(2L)BSC204* mutant R cells, the level of phosphorylated Moe in R-cell axonal terminals was significantly decreased. (D) R cells in C were double-stained with MAb 24B10. (E–H) The distribution of total Moe protein was visualized with anti-Moe antibody. (E) Moe was detected in wild-type R-cell bodies and axons. (F) R cells in E were double-stained with MAb 24B10. (G) In *sema1a^{P1}/Df(2L)BSC204* mutant R cells, the level of total Moe in R-cell axonal terminals was similar to that in wild type (E). (H) R cells in G were double-stained with MAb 24B10. (I) The relative level of phosphorylated Moe was quantified ($n = 10$). Loss of *sema1a* significantly decreased the level of phosphorylated Moe in R-cell axonal terminals ($P = 0.0045$). (J) The relative level of total Moe was quantified ($n > 16$). Loss of *sema1a* did not significantly affect the level of total Moe in R-cell axonal terminals ($P > 0.05$). ns, not significant. (K–N) R-cell axonal projection pattern was visualized with MAb 24B10 staining. (K) Wild type. (L) *sema1a^{P1}/Df(2L)BSC204* mutants. The arrows indicate gaps at the lamina termination layer. (M) *moe^{G0323}* mutants frequently displayed gaps (arrows) at the lamina termination layer, a phenotype similar to that in *sema1a* mutants (L). (N) Eye-specific knockdown of *moe* also caused the appearance of gaps (arrows) at the lamina termination layer. (Scale bar: A–H, 10 μ m; K–N, 20 μ m.) Error bars: SEM.

NCAM is tightly controlled to ensure proper development of the nervous system. For example, the expression of Fas2 is negatively regulated by the transcriptional factor Adf-1 in regulating dendrite development (17). In mammals, it is reported that removal of the polysialic-acid moiety of NCAM plays an important role in upregulating NCAM-mediated neurite–neurite adhesion during development (18).

We favor the model in which PlexA-Sema1a reverse signaling upregulates the function of Fas2 in mediating axon–axon association for circuit development in the visual system for the following reasons. First, PlexA, Sema1a, and Fas2 are expressed and genetically required in R-cell axons (3, 8) (Fig. 3 and *SI Appendix*, Fig. S4). Second, overexpression of PlexA, Sema1a, or Fas2 causes similar hyper-fasciculation of R-cell axons (3, 8) (*SI Appendix*, Fig. S6). And third, loss of *PlexA*, *Sema1a*, or *Fas2* causes dispersed distribution of R-cell axonal terminals and frequent appearance of gaps in the target region (8) (*SI Appendix*, Fig. S4). However, our current data cannot completely exclude an additional role of Sema1a in target recognition. It remains possible that, in addition to promoting Fas2-mediated R-cell axon–axon attraction, Sema1a reverse signaling also regulates interactions between R-cell axons and their target regions for visual circuit assembly.

The Rho-family small GTPase Rho1 appears to be a key target of Sema1a reverse signaling in regulating the function of Fas2. Our previous study from genetic analysis suggests a role for Sema1a in negatively regulating the function of Rho1 in the developing *Drosophila* visual system (8). In the present study, we show that Sema1a decreases the level of active Rho1. Moreover, Fas2-mediated cell–cell adhesion is enhanced by reducing the activity of Rho1 and inhibited by increasing the activity of Rho1. Together, these results establish a key role for negative regulation of Rho1 by Sema1a reverse signaling in upregulating Fas2.

That Rho1 promotes intracellular trafficking and degradation of Fas2 in cultured cells suggests that upregulation of Fas2 surface level by Sema1a-mediated inhibition of Rho1 is a possible mechanism for promoting Fas2-mediated axon–axon attraction. However, no obvious change in Fas2 level in R1–R6 terminals was detected in *sema1a* mutants. One possible explanation for this discrepancy is that, due to technical limitation, we could measure only the level of total Fas2, but not surface Fas2, in R-cell axonal terminals. Another possibility is that upregulation of Fas2 is transient, which makes it difficult to detect a change in Fas2 expression level when Sema1a is manipulated. It also remains possible that inhibition of Rho1 by Sema1a reverse signaling may increase both surface level and binding activity of Fas2. Future studies will be needed to address these possibilities.

In addition to the role of Rho1 in the Sema1a reverse-signaling pathway in the visual system, a recent study by Kolodkin and colleagues shows that Sema1a reverse signaling also regulates Rho1 in *Drosophila* motor axon guidance (6). The difference between photoreceptor and motor axons in the modulation of Rho1 by Sema1a reverse signaling may account for distinct effects on axon–axon interactions. Although negative regulation of Rho1 by Sema1a reverse signaling promotes axon–axon association in the visual system, Sema1a reverse signaling activates Rho1 in motor axons leading to axon–axon repulsion. One likely explanation is that Sema1a uses different downstream effectors to modulate Rho1 in different cell types. Whereas Moe is activated by Sema1a in photoreceptor axons, Pebble and RhoGAPp190 appear to link Sema1a reverse signaling with the modulation of Rho1 activity in motor axons (6). It remains unknown how Sema1a-induced changes in Rho1 activity modulate cell-surface adhesiveness leading to axon–axon repulsion in motor axon guidance.

Previous studies identify Moe as a negative regulator of Rho1 in epithelial morphogenesis (13). In this study, we provide several lines of evidence supporting that Sema1a negatively regulates the activity of Rho1 in R-cell axons by upregulating Moe. First, Moe interacts genetically with Sema1a in regulating R-cell axonal projections. Second, Sema1a associates with Moe and is required for the phosphorylation and activation of Moe in R-cell axons.

And third, like *Sema1a*, *Moe* displays a similar effect on the level of active *Rho1* in R-cell axons. The association of *Moe* with *Sema1a* may bring *Moe* in close proximity to its upstream kinase, thus facilitating the phosphorylation and activation of *Moe*. Thus, overexpression of *Sema1a* may allow the recruitment and activation of sufficient *Moe* protein in R-cell axons in a *PlexA*-independent manner, which upregulates the adhesive activity and/or stability of *Fas2* by inhibiting *Rho1*. In addition to its interaction with *Sema1a*, *Moe* is recently reported to interact with the tumor necrosis factor receptor *Wengen* in regulating R8 photoreceptor axon targeting (19). *Moe* may be a common target of multiple receptors to regulate different processes in circuit development.

In conclusion, our present study supports a model in which *Sema1a* reverse signaling negatively regulates the activity of *Rho1* and thus promotes *Fas2*-mediated axon-axon attraction in the *Drosophila* visual system. It will be of interest to determine if transmembrane Semaphorins in vertebrates also function similarly in regulating axon-axon interactions.

Materials and Methods

Genetics. To overexpress *Fas2* in R cells, *UAS-Fas2-yfp* flies (20) were crossed with *GMR-GAL4* or *GMR-GAL4, UAS-sema1a* flies. To knock down the level of *Fas2* in R cells, *UAS-Fas2-RNAi* (BDS#34084) flies were crossed with *GMR-GAL4* flies. Large clones (>50% of retina) of homozygous *Fas2^{EB112}* mutant tissues were generated in an otherwise heterozygous or wild-type eye by eye-specific mitotic recombination using the *eyFLP/FRT* system (21). To knock down the level of *Moe* in R cells, *UAS-moe-RNAi* flies (Bloomington *Drosophila* Stock Center #33936) were crossed with *GMR-GAL4* flies. To overexpress *Moe* in R cells, *UAS-moe-myc* flies (22) were crossed with *GMR-GAL4* or *GMR-GAL4, UAS-sema1a* flies. To express PKN-GFP in wild-type and *sema1a*-overexpression R cells, *UAS-Pkn-gfp* flies (10) were crossed with wild-type or *GMR-GAL4, UAS-sema1a* flies, respectively. To express PKN-GFP in *sema1a* mutant R cells, *GMR-GAL4, sema1a^{P1}/CyO; UAS-Pkn-gfp* flies were crossed with *Df(2L)BSC204/CyO-gfp*.

Molecular Biology. To generate *UAS-Fas2-yfp*, the DNA fragment containing the *Fas2-yfp* sequence was amplified from flies carrying the *UAS-Fas2-yfp* transgene (20) by PCR and subcloned into pCR2.1 vector. A *NotI/KpnI* fragment of the resulting plasmid was then subcloned into pUAST. To generate *UAS-sema1a-rfp* and *UAS-sema1a-venus*, the DNA sequence encoding *Sema1a* was amplified from *UAS-sema1a* by PCR and subcloned into pTWR and pTWV [*Drosophila* Genetic Resource Center (DGRC)] by using the gateway system (Invitrogen), respectively. To generate *UAS-sema1a^{ΔCyto-venus}* and *UAS-sema1a^{ΔCyto-flag}*, the DNA sequence encoding the entire sequence of extracellular and transmembrane domains and 16-amino-acid cytoplasmic sequence following the transmembrane region was amplified

from the plasmid *UAS-sema1a* by PCR and subcloned into pTWV and pTWF (DGRC) by using the gateway system, respectively. To generate *GST-Cyto*, the sequence encoding the cytoplasmic domain of *Sema1a* was amplified from the plasmid *UAS-sema1a* by PCR and subcloned into the EcoRI/XhoI sites of pGEX-4T-1 vector. The *UAS-Pkn-gfp* plasmid was provided by António Jacinto (Universidade de Lisboa, Lisbon, Portugal) (10). To generate *UAS-moe-flag*, the DNA sequence encoding *Moe* was amplified from the plasmid DH0120 (provided by David R. Hipfner, Institut de Recherches Cliniques de Montréal, Montréal) by PCR and subcloned into the pTWF vector by using the gateway system. To generate *UAS-Rho1N19* and *UAS-Rho1V14*, the sequence was amplified from flies carrying *UAS-Rho1.N19* and *UAS-Rho1.V14* transgenes by PCR, respectively. The resulting fragment was then subcloned into the EcoRI/XhoI sites of pUAST vector.

Immunostaining. Dissection and immunostaining of the eye-brain complexes from third-instar larvae were performed as described previously (23). Antibodies were used at the following dilutions: MAB24B10 [1:100; Developmental Studies Hybridoma Bank (DSHB)], mouse anti-*Fas2* 1D4 [1:100; DSHB], rabbit anti-*Moe* (1:20,000; provided by D. Hipfner), rabbit anti-pMoe (1:200; Cell Signaling Technology), mouse anti-Dynamin (1:500; BD Biosciences), and rat anti-HA (1:3,000; Roche). Cultured S2 cells were labeled with CellMask Deep Red Plasma Membrane Stains (1:2,000; Life Technologies) for 7 min to visualize plasma membrane. Dissociated R cells from third-instar larval eye discs were cultured and stained with antibodies similarly as described previously (24).

Cell-Cell Aggregation Assays. *Drosophila* S2 cells were cultured in EX-CELL 420 serum-free medium (Sigma-Aldrich) at 25 °C. Cell transfection and aggregation assays were performed similarly as described previously (25).

Biochemistry. Information about purification of GST and GST-*Sema1a^{Cyto}* fusion proteins, pull-down, and coimmunoprecipitation assays is described in *SI Appendix*.

Statistical Analysis. Student *t* test was used for statistical analysis. The difference is considered as significant when a *P* value is <0.05.

ACKNOWLEDGMENTS. We thank people in the Y.R. laboratory for comments and suggestions. We also thank Dr. P. Barker, Dr. H. Bellen, Dr. D. Hipfner, Dr. A. Jacinto, Dr. A. Nose, Dr. D. Ready, Dr. F. Shoenk, and Dr. S. Simões for reagents and fly stocks and the Bloomington Stock Center, the *Drosophila* Genomics Resource Center, and the Transgenic RNAi Project at Harvard Medical School (National Institutes of Health/National Institute of General Medical Sciences R01-GM084947). This work was supported by an operating grant (MOP-14688) from Canadian Institutes of Health Research (to Y.R.) and by a McGill University Health Centre studentship (to H.-H.H.).

1. Yazdani U, Terman JR (2006) The semaphorins. *Genome Biol* 7(3):211.
2. Mann F, Chauvet S, Rougon G (2007) Semaphorins in development and adult brain: Implication for neurological diseases. *Prog Neurobiol* 82(2):57–79.
3. Cafferty P, Yu L, Long H, Rao Y (2006) Semaphorin-1a functions as a guidance receptor in the *Drosophila* visual system. *J Neurosci* 26(15):3999–4003.
4. Komiyama T, Sweeney LB, Schuldiner O, Garcia KC, Luo L (2007) Graded expression of semaphorin-1a cell-autonomously directs dendritic targeting of olfactory projection neurons. *Cell* 128(2):399–410.
5. Godenschwege TA, Hu H, Shan-Crofts X, Goodman CS, Murphey RK (2002) Bi-directional signaling by Semaphorin 1a during central synapse formation in *Drosophila*. *Nat Neurosci* 5(12):1294–1301.
6. Jeong S, Juhaszova K, Kolodkin AL (2012) The control of semaphorin-1a-mediated reverse signaling by opposing pebble and RhoGAP190 functions in *Drosophila*. *Neuron* 76(4):721–734.
7. Toyofuku T, et al. (2004) Guidance of myocardial patterning in cardiac development by *Sema6D* reverse signalling. *Nat Cell Biol* 6(12):1204–1211.
8. Yu L, Zhou Y, Cheng S, Rao Y (2010) Plexin a-semaphorin-1a reverse signaling regulates photoreceptor axon guidance in *Drosophila*. *J Neurosci* 30(36):12151–12156.
9. Hadjiconomou D, Timofeev K, Salecker I (2011) A step-by-step guide to visual circuit assembly in *Drosophila*. *Curr Opin Neurobiol* 21(1):76–84.
10. Simões S, et al. (2006) Compartmentalisation of Rho regulators directs cell invagination during tissue morphogenesis. *Development* 133(21):4257–4267.
11. Ferguson SM, De Camilli P (2012) Dynamin, a membrane-remodelling GTPase. *Nat Rev Mol Cell Biol* 13(2):75–88.
12. Pfeiffer SR (2013) Rab GTPase regulation of membrane identity. *Curr Opin Cell Biol* 25(4):414–419.
13. Speck O, Hughes SC, Noren NK, Kulikauskas RM, Fehon RG (2003) Moesin functions antagonistically to the Rho pathway to maintain epithelial integrity. *Nature* 421(6918):83–87.
14. Hipfner DR, Keller N, Cohen SM (2004) Slik Sterile-20 kinase regulates Moesin activity to promote epithelial integrity during tissue growth. *Genes Dev* 18(18):2243–2248.
15. Kunda P, Pelling AE, Liu T, Baum B (2008) Moesin controls cortical rigidity, cell rounding, and spindle morphogenesis during mitosis. *Curr Biol* 18(2):91–101.
16. Hinsby AM, Berezin V, Bock E (2004) Molecular mechanisms of NCAM function. *Front Biosci* 9:2227–2244.
17. Timmerman C, et al. (2013) The *Drosophila* transcription factor Adf-1 (nalyot) regulates dendrite growth by controlling *FasII* and *Staufen* expression downstream of CaMKII and neural activity. *J Neurosci* 33(29):11916–11931.
18. Acheson A, Sunshine JL, Rutishauser U (1991) NCAM polysialic acid can regulate both cell-cell and cell-substrate interactions. *J Cell Biol* 114(1):143–153.
19. Ruan W, Unsain N, Desbarats J, Fon EA, Barker PA (2013) *Wengen*, the sole tumour necrosis factor receptor in *Drosophila*, collaborates with moesin to control photoreceptor axon targeting during development. *PLoS ONE* 8(3):e60091.
20. Kohsaka H, Takasu E, Nose A (2007) In vivo induction of postsynaptic molecular assembly by the cell adhesion molecule Fasciclin2. *J Cell Biol* 179(6):1289–1300.
21. Newsome TP, Asling B, Dickson BJ (2000) Analysis of *Drosophila* photoreceptor axon guidance in eye-specific mosaics. *Development* 127(4):851–860.
22. Karagiannis SA, Ready DF (2004) Moesin contributes an essential structural role in *Drosophila* photoreceptor morphogenesis. *Development* 131(4):725–732.
23. Ruan W, Pang P, Rao Y (1999) The SH2/SH3 adaptor protein dock interacts with the Ste20-like kinase *misshapen* in controlling growth cone motility. *Neuron* 24(3):595–605.
24. Li C, Meinertzhagen IA (1995) Conditions for the primary culture of eye imaginal discs from *Drosophila melanogaster*. *J Neurobiol* 28(3):363–380.
25. Cameron S, et al. (2013) Visual circuit assembly requires fine tuning of the novel Ig transmembrane protein *Borderless*. *J Neurosci* 33(44):17413–17421.